JACS
JOURNAL OF THE AMERICAN CHEMICAL SOCIETY

COMMUNICATION

pubs.acs.org/JACS

Intermolecular Alignment in Y145Stop Human Prion Protein Amyloid Fibrils Probed by Solid-State NMR Spectroscopy

Jonathan J. Helmus,[†] Krystyna Surewicz,[‡] Marcin I. Apostol,[‡] Witold K. Surewicz,[‡] and Christopher P. Jaroniec*[,†]

[†]Department of Chemistry, The Ohio State University, Columbus, Ohio 43210, United States

[‡]Department of Physiology and Biophysics, Case Western Reserve University, Cleveland, Ohio 44106, United States

Supporting Information

ABSTRACT: The Y145Stop mutant of human prion protein, huPrP23−144, has been linked to PrP cerebral amyloid angiopathy, an inherited amyloid disease, and also serves as a valuable in vitro model for investigating the molecular basis of amyloid strains. Prior studies of huPrP23−144 amyloid by magic-angle-spinning (MAS) solid-state NMR spectroscopy revealed a compact β-rich amyloid core region near the C-terminus and an unstructured N-terminal domain. Here, with the focus on understanding the higher-order architecture of huPrP23−144 fibrils, we probed the intermolecular alignment of β-strands within the amyloid core using MAS NMR techniques and fibrils formed from equimolar mixtures of ^{15}N-labeled protein and ^{13}C-huPrP23−144 prepared with [1,3-$^{13}C_2$] or [2-^{13}C]glycerol. Numerous intermolecular correlations involving backbone atoms observed in 2D ^{15}N−^{13}C spectra unequivocally suggest an overall parallel in-register alignment of the β-sheet core. Additional experiments that report on intermolecular ^{15}N−^{13}CO and ^{15}N−^{13}Cα dipolar couplings yielded an estimated strand spacing that is within ∼10% of the distances of 4.7−4.8 Å typical for parallel β-sheets.

Conformational conversion of the prion protein (PrP) to ordered β-sheet-rich amyloid-like aggregates is associated with the pathogenesis of a group of fatal neurodegenerative diseases known as transmissible spongiform encephalopathies.[1] Although once controversial, the notion that prions can propagate via a "protein-only" mechanism with the misfolded aggregates acting as self-replicating infectious agents is becoming widely accepted, particularly in light of recent findings that infectious particles can be generated in vitro from purified PrP[2] and observations regarding conformation-based inheritance in fungi.[3] While the ability of prions to propagate appears to be encoded in the three-dimensional (3D) structure of PrP aggregates, the molecular mechanisms underlying this phenomenon are currently not well understood in atomic-level detail.[4]

The C-terminally truncated Y145Stop variant of human PrP (huPrP23−144) is associated with a heritable cerebral amyloid angiopathy.[5] Though this type of prionopathy appears to be noninfectious, we have previously shown that huPrP23−144 provides a valuable model in vitro for studying the molecular basis of amyloid formation as well as the phenomena of amyloid strains and seeding specificity.[6] More recently, we initiated multidimensional magic-angle-spinning (MAS) solid-state NMR studies of the structure and conformational dynamics of amyloid fibrils prepared from recombinant ^{13}C,^{15}N-enriched huPrP23−144.[7,8] These studies revealed that huPrP23−144 fibrils contain a relatively rigid amyloid core region composed of only ∼30 C-terminal amino acids (aa), with many residues in a β-conformation. In contrast, a large N-terminal domain comprising aa ∼23−111 was found to be a highly flexible ensemble of random-coil-like conformers.

Here, with the emphasis on gaining insight into the higher-order structure of huPrP23−144 fibrils, we probed the intermolecular alignment of β-strands in the amyloid core region by MAS solid-state NMR spectroscopy. Solid-state NMR methods are uniquely well-suited for this type of analysis and have previously been used to investigate the core architectures of numerous peptide-derived fibrils,[9] such as β-amyloid[10] and fragments of amylin,[11] transthyretin[12] and β_2-microglobulin,[13] as well as several larger proteins or protein domains,[9] including Sup35p-(1−253),[14] Ure2p,[15] β_2-microglobulin,[16] HET-s(218−289),[17] and HET-s.[18] In this study, we utilized transferred-echo double resonance (TEDOR) NMR techniques[19,20] and fibril samples prepared from equimolar mixtures of ^{15}N-huPrP23−144 and sparsely ^{13}C-labeled huPrP23−144 to record 2D ^{15}N−^{13}C chemical shift correlation spectra containing a large number of intermolecular correlations involving the backbone ^{15}N, ^{13}CO, and ^{13}Cα nuclei. We also evaluated the magnitudes of intermolecular ^{15}N−^{13}CO and ^{15}N−^{13}Cα dipolar couplings, which report on the strand spacing within the β-sheet core.

The huPrP23−144 amyloid fibril samples were grown in pH 6.4 phosphate buffer from physical mixtures of ^{15}N- and ^{13}C-labeled monomers in a 1:1 molar ratio, where the ^{13}C-labeled proteins were generated using [1,3-$^{13}C_2$] or [2-^{13}C]glycerol-based expression media[21,22] [see the Supporting Information (SI) for details]. This type of ^{13}C enrichment, which removes many one-bond ^{13}C−^{13}C dipolar and J couplings and leads to improved spectral resolution and higher magnetization transfer efficiencies,[22,23] is particularly beneficial in the context of ^{15}N−^{13}C TEDOR experiments.[16,24] In addition to the mixed 1,3-$^{13}C_2$/^{15}N and 2-^{13}C/^{15}N huPrP23−144 fibrils, we also prepared control amyloid samples from pure 1,3-$^{13}C_2$,^{15}N- and 2-^{13}C,^{15}N-labeled huPrP23−144 as well as 1,3-$^{13}C_2$,^{15}N- and 2-^{13}C,^{15}N- huPrP23−144 diluted in natural-abundance (^{12}C,^{14}N) protein in a 1:3 molar ratio.

For the undiluted and diluted 1,3-$^{13}C_2$,^{15}N- and 2-^{13}C,^{15}N-labeled control amyloid samples, application of the z-filtered

Received: July 12, 2011
Published: August 10, 2011

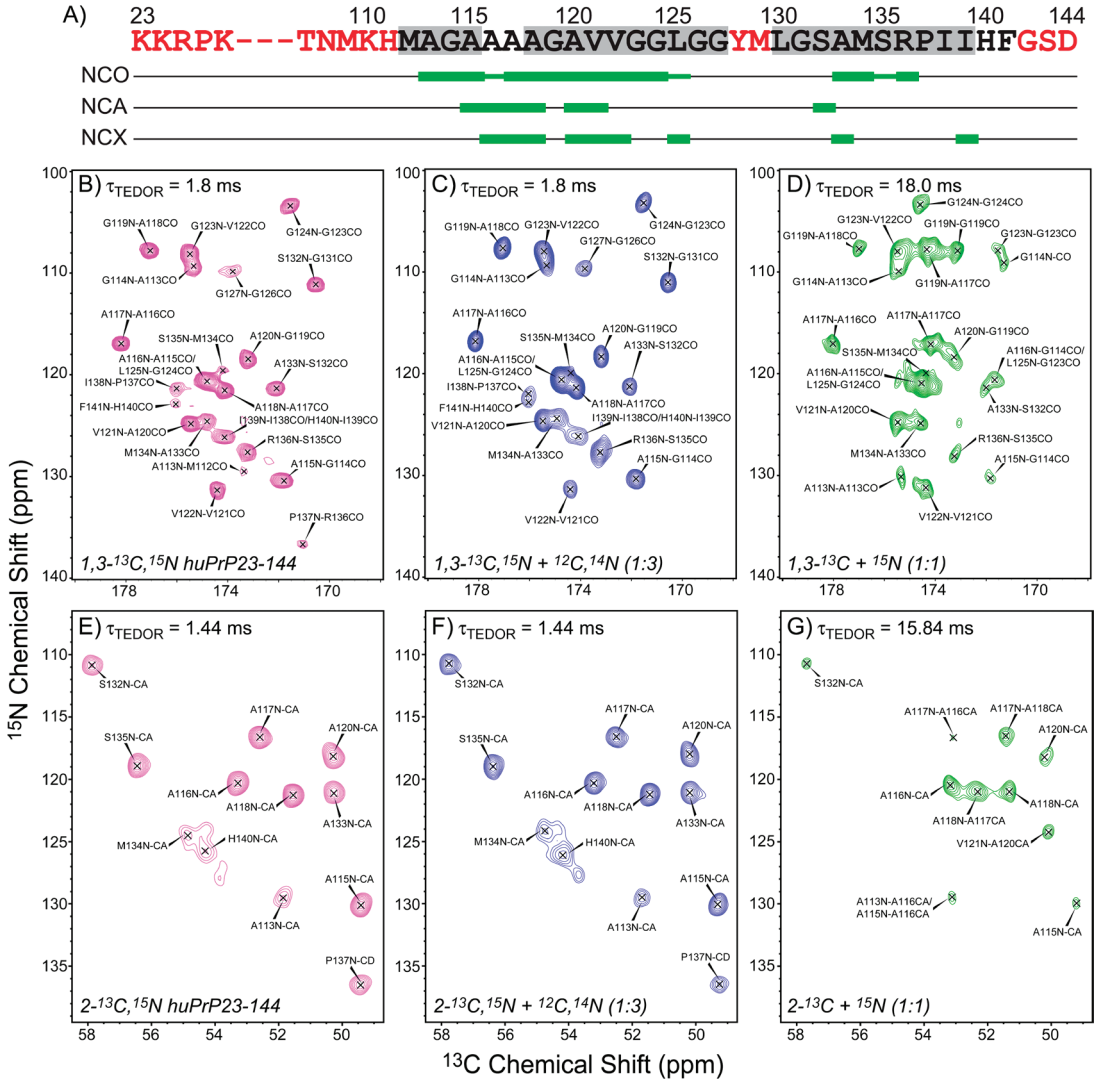

Figure 1. (A) Partial amino acid sequence of huPrP23−144. Residues exhibiting significant conformational dynamics are shown in red font and relatively rigid amyloid core residues in black font,[7,8] and the three β-strand segments predicted using TALOS+[25] are highlighted by gray shading. Also shown is a summary of the intermolecular $^{15}N-^{13}C$ correlations observed in *z*-filtered TEDOR spectra recorded for the mixed 1,3-$^{13}C_2$/^{15}N- and 2-^{13}C/^{15}N huPrP23−144 fibril samples (panels D and G; also see Figure S1C). Thick green rectangles under residue *i* indicate than an unambiguous intermolecular $^{15}N-^{13}C$ correlation was observed between the amide ^{15}N of residue *i* and $^{13}CO_{i-1}$ and/or $^{13}CO_i$ (NCO), $^{13}C\alpha_{i-1}$ and/or $^{13}C\alpha_i$ (NCA), and side-chain ^{13}C of residue *i* (NCX). Narrow green rectangles correspond to ambiguous intermolecular $^{15}N-^{13}C$ correlations. (B−D) $^{15}N-^{13}CO$ (NCO) correlation spectra of huPrP23−144 amyloid fibrils recorded at an ^1H frequency of 500 MHz, a MAS rate of 11.111 kHz, and an effective sample temperature of ∼5 °C using the *z*-filtered TEDOR pulse scheme[20] ($^{15}N-^{13}C$ dipolar mixing times, τ_{TEDOR}, are indicated in the spectra). The fibril samples were prepared from (B) 1,3-$^{13}C_2$,^{15}N-huPrP23−144, (C) a mixture of 1,3-$^{13}C_2$,^{15}N-huPrP23−144 and natural-abundance (^{12}C,^{14}N) huPrP23−144 in a 1:3 molar ratio, and (D) a mixture of 1,3-$^{13}C_2$-huPrP23−144 and ^{15}N-huPrP23−144 in a 1:1 molar ratio. The experiment times for the spectra in (B−D) were ∼14, ∼27, and ∼212 h, respectively. (E−G) Similar to (B−D) but for $^{15}N-^{13}C\alpha$ (NCA) spectra and fibril samples grown from huPrP23−144 prepared using [2-^{13}C] instead of [1,3-$^{13}C_2$]glycerol. The experiment times were ∼7, ∼27, and ∼216 h, respectively.

TEDOR pulse sequence[20] with short mixing times ($\tau_{TEDOR} \approx$ 1.5−2 ms) and without ^{15}N evolution yielded spectra displaying $^{13}CO/^{13}C\alpha$ intensities that are ∼20−25% of those obtained for the corresponding cross-polarization (CP) reference ^{13}C spectra, indicating magnetization transfer via strong ∼1 kHz one-bond $^{15}N-^{13}C$ dipolar couplings. In contrast, no appreciable intensity was obtained for mixed 1,3-$^{13}C_2$/^{15}N and 2-^{13}C/^{15}N fibrils under the same experimental conditions (see the TEDOR trajectories in Figure 2), confirming that contributions to the spectra from one-bond $^{15}N-^{13}C$ couplings involving the ∼1% of natural-abundance ^{13}C atoms in ^{15}N-huPrP23−144 are negligible, obviating the need to prepare mixed $^{13}C/^{15}N$ fibril samples containing specifically ^{13}C-depleted, ^{15}N-labeled protein. The use of longer TEDOR mixing times (on the order of 15−20 ms), however, resulted in a clear buildup of $^{13}CO/^{13}C\alpha$ intensities up to 2−4% of those found in CP spectra. The latter finding is consistent with magnetization transfer via weak intermolecular $^{15}N-^{13}C$ dipolar couplings corresponding to distances in the 4−5 Å regime (see discussion below), associated with neighboring ^{15}N- and 1,3-$^{13}C_2$- or 2-^{13}C-labeled huPrP23−144 molecules in the fibril lattice.

In order to identify the specific protein sites responsible for the intermolecular backbone $^{15}N-^{13}C$ contacts, we recorded a series of 2D $^{15}N-^{13}CO$ (NCO) and $^{15}N-^{13}C\alpha$ (NCA) TEDOR chemical shift correlation spectra for different huPrP23−144

dx.doi.org/10.1021/ja206469q |*J. Am. Chem. Soc.* 2011, 133, 13934–13937

fibril samples (Figure 1). The short-mixing-time reference NCO and NCA spectra for 1,3-$^{13}C_2$,^{15}N- and 2-^{13}C,^{15}N-labeled fibrils, respectively, contained exclusively intramolecular one-bond $^{15}N-^{13}CO$ and $^{15}N-^{13}C\alpha$ correlations, which could be readily identified on the basis of previous assignments established for uniformly ^{13}C,^{15}N-enriched huPrP23−144 amyloid.[7] Moreover, the fact that pairs of spectra for corresponding undiluted/diluted fibrils were effectively identical indicates the high reproducibility of the sample preparation protocols and experiments employed in this study.

The NCO and NCA spectra for mixed 1,3-$^{13}C_2$/^{15}N and 2-^{13}C/^{15}N huPrP23−144 fibrils (Figure 1D,G) were recorded with TEDOR mixing times of 18 and 15.84 ms, respectively. Together, these two spectra contain ∼30 relatively intense correlations involving the backbone atoms for the amyloid core residues, with ^{15}N, ^{13}CO, and $^{13}C\alpha$ frequencies closely matching those observed for the control 1,3-$^{13}C_2$,^{15}N- and 2-^{13}C,^{15}N-labeled samples. The NCO data set contains a significantly greater number of cross-peaks relative to NCA, most likely as a result of more favorable transverse relaxation properties for ^{13}CO versus $^{13}C\alpha$ nuclei and larger magnitudes of $^{15}N-^{13}C$ dipolar couplings. A careful inspection of these data reveals that the majority of resonances present in the NCO and NCA spectra result from intermolecular $^{15}N_i-^{13}CO_{i-1}$ and $^{15}N_i-^{13}C\alpha_i$ transfers, respectively, with most of the remaining cross-peaks corresponding to $^{15}N_i-^{13}CO_i$ and $^{15}N_i-^{13}C\alpha_{i-1}$ transfers, respectively. In addition, a set of $^{15}N-^{13}CX$ (NCX) TEDOR spectra containing correlations involving side-chain ^{13}C methyl groups was recorded for fibrils grown from ^{13}C or ^{13}C,^{15}N proteins prepared using the [1,3-$^{13}C_2$]glycerol labeling scheme (Figure S1 in the SI). The spectrum for mixed 1,3-$^{13}C_2$/^{15}N fibrils displays 10 intermolecular $^{15}N_i-^{13}C_i$ cross-peaks, which further support the correlations detected in the NCO and NCA spectra. A graphical summary of the correlations observed in the NCO, NCA, and NCX spectra (Figure 1C) shows the presence of intermolecular contacts for the vast majority of residues within the ∼113−125 region (which constitutes the most rigid part of the amyloid core[8]) as well as multiple residues in the C-terminal β-strand (aa ∼132−139).

As noted above, the long-mixing-time TEDOR experiments for the mixed ^{13}C/^{15}N fibrils report exclusively on intermolecular contacts. Furthermore, any contributions to the spectra arising from intramolecular $^{15}N-^{13}C$ couplings involving residual ^{13}C nuclei present at natural abundance in ^{15}N-huPrP23−144 are below the detection limit of the measurements, a notion further supported by the fact that a number of correlations that would normally be observed if such natural abundance background effects were significant are missing in the 2D $^{15}N-^{13}C$ spectra in Figure 1 and Figure S1 (e.g., G124N−G123CO, S132N−G131CO, A133N−Cα, A115N−Cβ, etc.). Thus, the present data strongly indicate that β-strands in the core region of huPrP23−144 amyloid fibrils are organized in a parallel in-register fashion. Within this structural model, the nearest-neighbor and next-nearest-neighbor backbone $^{15}N-^{13}CO$ and $^{13}C\alpha$ distances correspond to $^{15}N_i-^{13}CO_{i-1}$ (∼4.2 Å)/$^{15}N_i-^{13}CO_i$ (5.2−5.4 Å) and $^{15}N_i-^{13}C\alpha_i$ (4.7−4.8 Å)/$^{15}N_i-^{13}C\alpha_{i-1}$ (5.2−5.4 Å), respectively (Figure S2), consistent with the correlations observed in the NCO and NCA spectra.

Although the limited sensitivity of TEDOR experiments for mixed ^{13}C/^{15}N fibrils precluded the determination of intermolecular $^{15}N-^{13}C$ distances in a residue-specific fashion, we were able to estimate the spacing between adjacent huPrP23−144 molecules

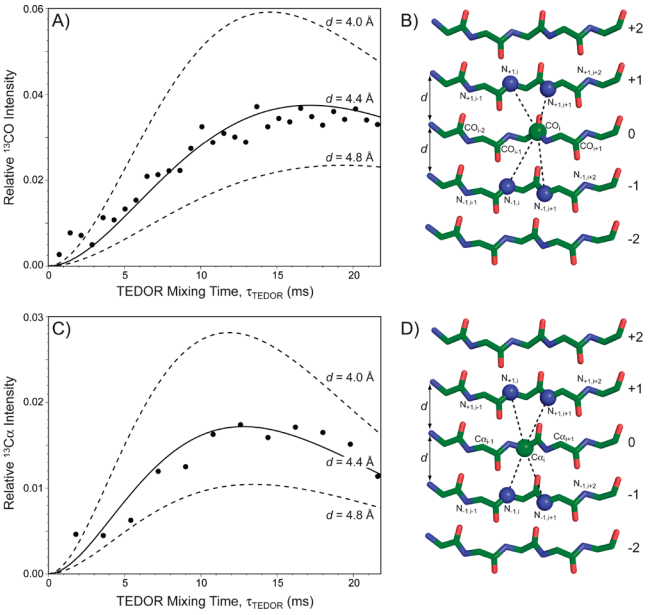

Figure 2. (A, C) Experimental (points) and simulated (lines) 1D TEDOR trajectories that report simultaneously on all intermolecular (A) $^{15}N-^{13}CO$ and (C) $^{15}N-^{13}C\alpha$ distances in huPrP23−144 amyloid fibrils. The experimental trajectories in (A) and (C) were recorded for the mixed 1,3-$^{13}C_2$/^{15}N and 2-^{13}C/^{15}N fibril samples, respectively, as described in the SI, and the ^{13}CO and $^{13}C\alpha$ intensities in the plots have been scaled by the corresponding intensities in CP ^{13}C reference spectra recorded under identical conditions. The total experiment times were ∼41 and ∼68 h, respectively. (B, D) Model spin systems, based on the X-ray structure of amyloid-like microcrystals of the peptide GNNQQNY[26] displaying a parallel in-register alignment of the β-strands (PDB entry 2OMM), that were used to generate the simulated TEDOR trajectories corresponding to the experimental data in (A) and (C), respectively, within the SPINEVOLUTION software.[27] The atoms included in the simulations are indicated by spheres. The simulated trajectories were generated as described in detail in the SI as a function of a single distance parameter d corresponding to the spacing (in Å) between adjacent β-strands as indicated in the structural models. The best-fit $^{15}N-^{13}CO$ and $^{15}N-^{13}C\alpha$ simulations, corresponding to d = 4.4 Å, are shown as solid lines, and simulations for d values varying by ±10% from the best-fit value are shown as dashed lines.

in the β-sheet core by recording 1D TEDOR trajectories that simultaneously report on all $^{15}N-^{13}CO$ or $^{15}N-^{13}C\alpha$ dipolar couplings (with the main contributions to the trajectories arising from the strongest $^{15}N_i-^{13}CO_{i-1}$ and $^{15}N_i-^{13}C\alpha_i$ cross-peaks in the 2D spectra in Figure 1). These trajectories, which are shown in Figure 2, were simulated as a function of intermolecular spacing as described in detail in the SI by considering all $^{15}N-^{13}CO/^{13}C\alpha$ distances of <6 Å within the parallel in-register model expected for the mixed ^{13}C/^{15}N fibril samples and assuming these distances to be the same for all residues. The calculated $^{15}N-^{13}CO$ and $^{15}N-^{13}C\alpha$ trajectories are in good agreement with their experimental counterparts, and both data sets yield a self-consistent estimate of d = 4.4 Å for the β-strand spacing. Although this estimated value is somewhat less than that expected considering typical hydrogen-bond topologies in parallel β-sheets, it falls within ∼10% of the canonical 4.7−4.8 Å strand spacings typically observed for this motif. The interstrand spacing for huPrP23−144 amyloid fibrils as determined by fiber X-ray diffraction is 4.65 Å (Figure S3). Relatively small underestimation of this value by simulations of TEDOR trajectories is

not entirely surprising given that, due to relatively small magnitudes of the $^{15}N-^{13}C$ couplings, such simulations depend to some degree on additional parameters such as the effective transverse ^{13}C spin relaxation rate during TEDOR mixing and overall spectral amplitude scaling.[20] In this study, we made an attempt to eliminate the dependence of data modeling on these extra parameters by using reference experiments as described in the SI. However, it should be noted that when values for the relaxation and scaling parameters that differed somewhat from those determined in the reference experiments were used, good agreement between the experimental and simulated trajectories could also be obtained for intermolecular spacings in the range of 4.5−5 Å.

In conclusion, the wealth of site-resolved solid-state NMR data presented here for fibrils prepared from highly ^{13}C- and ^{15}N-enriched protein molecules establish rather unequivocally that the huPrP23−144 β-sheet core displays an overall parallel in-register alignment. While given the $^{15}N-^{13}C$ correlations observed in 2D TEDOR spectra it is possible that several residues at the edges of β-strands have geometries that locally deviate from an ideal parallel in-register β-sheet arrangement, our experiments clearly rule out the existence of other topologies such as antiparallel β-sheets and parallel β-sheet motifs displaying a uniform registry shift of one or more residues. A parallel in-register β-structure has been observed for many other amyloidogenic polypeptides.[9] A similar arrangement has also been found for fibrils formed by full-length PrP and PrP fragment 90−231,[28,29] even though the residues forming the β-core of the latter amyloids (aa ∼160−220)[28] are different from those encompassing the β-strands in huPrP23−144. The fundamental insights into the intermolecular arrangement of β-strands in human PrP23−144 fibrils gained from the present study provide a stepping stone toward the construction of high-resolution structural models and full understanding of the molecular basis of PrP23−144 amyloid strains and their seeding specificities.

■ ASSOCIATED CONTENT

Supporting Information. Experimental and data analysis sections, NMR and fiber X-ray diffraction data, and structural models. This material is available free of charge via the Internet at http://pubs.acs.org.

■ AUTHOR INFORMATION

Corresponding Author
jaroniec@chemistry.ohio-state.edu

■ ACKNOWLEDGMENT

This work was supported by grants from the National Institutes of Health (R01GM094357 to C.P.J. and R01NS038604 and R01NS044158 to W.K.S.).

■ REFERENCES

(1) (a) Prusiner, S. B. *Proc. Natl. Acad. Sci. U.S.A.* **1998**, *95*, 13363. (b) Caughey, B.; Chesebro, B. *Adv. Virus Res.* **2001**, *56*, 277. (c) Collinge, J. *Annu. Rev. Neurosci.* **2001**, *24*, 519.

(2) (a) Legname, G.; Baskakov, I. V.; Nguyen, H. O.; Riesner, D.; Cohen, F. E.; DeArmond, S. J.; Prusiner, S. B. *Science* **2004**, *305*, 673. (b) Deleault, N. R.; Harris, B. T.; Rees, J. R.; Supattapone, S. *Proc. Natl. Acad. Sci. U.S.A.* **2007**, *104*, 9741. (c) Wang, F.; Wang, X.; Yuan, C. G.; Ma, J. *Science* **2010**, *327*, 1132. (d) Kim, J. I.; Cali, I.; Surewicz, K.; Kong, Q.; Raymond, G. J.; Atarashi, R.; Race, B.; Qing, L.; Gambetti, P.; Caughey, B.; Surewicz, W. K. *J. Biol. Chem.* **2010**, *285*, 14083.

(3) (a) Chien, P.; Weissman, J. S.; DePace, A. H. *Annu. Rev. Biochem.* **2004**, *73*, 617. (b) Wickner, R. B.; Edskes, H. K.; Roberts, B. T.; Baxa, U.; Pierce, M. M.; Ross, E. D.; Brachmann, A. *Genes Dev.* **2004**, *18*, 470.

(4) (a) Collinge, J.; Clarke, A. R. *Science* **2007**, *318*, 930. (b) Aguzzi, A.; Sigurdson, C.; Heikenwaelder, M. *Annu. Rev. Pathol.* **2008**, *3*, 11. (c) Cobb, N. J.; Surewicz, W. K. *Biochemistry* **2009**, *48*, 2574.

(5) Ghetti, B.; Tagliavini, F.; Takao, M.; Bugiani, O.; Piccardo, P. *Clin. Lab. Med.* **2003**, *23*, 65.

(6) (a) Kundu, B.; Maiti, N. R.; Jones, E. M.; Surewicz, K. A.; Vanik, D. L.; Surewicz, W. K. *Proc. Natl. Acad. Sci. U.S.A.* **2003**, *100*, 12069. (b) Vanik, D. L.; Surewicz, K. A.; Surewicz, W. K. *Mol. Cell* **2004**, *14*, 139. (c) Jones, E. M.; Surewicz, W. K. *Cell* **2005**, *121*, 63.

(7) Helmus, J. J.; Surewicz, K.; Nadaud, P. S.; Surewicz, W. K.; Jaroniec, C. P. *Proc. Natl. Acad. Sci. U.S.A.* **2008**, *105*, 6284.

(8) Helmus, J. J.; Surewicz, K.; Surewicz, W. K.; Jaroniec, C. P. *J. Am. Chem. Soc.* **2010**, *132*, 2393.

(9) Tycko, R. *Annu. Rev. Phys. Chem.* **2011**, *62*, 279.

(10) (a) Benzinger, T. L. S.; Gregory, D. M.; Burkoth, T. S.; Miller-Auer, H.; Lynn, D. G.; Botto, R. E.; Meredith, S. C. *Proc. Natl. Acad. Sci. U.S.A.* **1998**, *95*, 13407. (b) Petkova, A. T.; Ishii, Y.; Balbach, J. J.; Antzutkin, O. N.; Leapman, R. D.; Delaglio, F.; Tycko, R. *Proc. Natl. Acad. Sci. U.S.A.* **2002**, *99*, 16742.

(11) Madine, J.; Jack, E.; Stockley, P. G.; Radford, S. E.; Serpell, L. C.; Middleton, D. A. *J. Am. Chem. Soc.* **2008**, *130*, 14990.

(12) Caporini, M. A.; Bajaj, V. S.; Veshtort, M.; Fitzpatrick, A.; MacPhee, C. E.; Vendruscolo, M.; Dobson, C. M.; Griffin, R. G. *J. Phys. Chem. B* **2010**, *114*, 13555.

(13) Iwata, K.; Fujiwara, T.; Matsuki, Y.; Akutsu, H.; Takahashi, S.; Naiki, H.; Goto, Y. *Proc. Natl. Acad. Sci. U.S.A.* **2006**, *103*, 18119.

(14) Shewmaker, F.; Wickner, R. B.; Tycko, R. *Proc. Natl. Acad. Sci. U.S.A.* **2006**, *103*, 19754.

(15) (a) Loquet, A.; Bousset, L.; Gardiennet, C.; Sourigues, Y.; Wasmer, C.; Habenstein, B.; Schütz, A.; Meier, B. H.; Melki, R.; Böckmann, A. *J. Mol. Biol.* **2009**, *394*, 108. (b) Kryndushkin, D. S.; Wickner, R. B.; Tycko, R. *J. Mol. Biol.* **2011**, *409*, 263.

(16) (a) Debelouchina, G. T.; Platt, G. W.; Bayro, M. J.; Radford, S. E.; Griffin, R. G. *J. Am. Chem. Soc.* **2010**, *132*, 17077. (b) Bayro, M. J.; Debelouchina, G. T.; Eddy, M. T.; Birkett, N. R.; MacPhee, C. E.; Rosay, M. M.; Maas, W. E.; Dobson, C. M.; Griffin, R. G. *J. Am. Chem. Soc.* **2011**, in press, DOI: 10.1021/ja203756x.

(17) (a) Wasmer, C.; Lange, A.; Van Melckebeke, H.; Siemer, A. B.; Riek, R.; Meier, B. H. *Science* **2008**, *319*, 1523. (b) Van Melckebeke, H.; Wasmer, C.; Lange, A.; AB, E.; Loquet, A.; Böckmann, A.; Meier, B. H. *J. Am. Chem. Soc.* **2010**, *132*, 13765.

(18) Wasmer, C.; Schütz, A.; Loquet, A.; Buhtz, C.; Greenwald, J.; Riek, R.; Böckmann, A.; Meier, B. H. *J. Mol. Biol.* **2009**, *394*, 119.

(19) Hing, A. W.; Vega, S.; Schaefer, J. *J. Magn. Reson.* **1992**, *96*, 205.

(20) Jaroniec, C. P.; Filip, C.; Griffin, R. G. *J. Am. Chem. Soc.* **2002**, *124*, 10728.

(21) LeMaster, D. M.; Kushlan, D. M. *J. Am. Chem. Soc.* **1996**, *118*, 9255.

(22) Castellani, F.; van Rossum, B.; Diehl, A.; Schubert, M.; Rehbein, K.; Oschkinat, H. *Nature* **2002**, *420*, 98.

(23) Bayro, M. J.; Maly, T.; Birkett, N. R.; Dobson, C. M.; Griffin, R. G. *Angew. Chem., Int. Ed.* **2009**, *48*, 5708.

(24) Nieuwkoop, A. J.; Wylie, B. J.; Franks, W. T.; Shah, G. J.; Rienstra, C. M. *J. Chem. Phys.* **2009**, *131*, No. 095101.

(25) Shen, Y.; Delaglio, F.; Cornilescu, G.; Bax, A. *J. Biomol. NMR* **2009**, *44*, 213.

(26) Sawaya, M. R.; Sambashivan, S.; Nelson, R.; Ivanova, M. I.; Sievers, S. A.; Apostol, M. I.; Thompson, M. J.; Balbirnie, M.; Wiltzius, J. J.; McFarlane, H. T.; Madsen, A. Ø.; Riekel, C.; Eisenberg, D. *Nature* **2007**, *447*, 453.

(27) Veshtort, M.; Griffin, R. G. *J. Magn. Reson.* **2006**, *178*, 248.

(28) Cobb, N. J.; Sonnichsen, F. D.; McHaourab, H.; Surewicz, W. K. *Proc. Natl. Acad. Sci. U.S.A.* **2007**, *104*, 18946.

(29) Tycko, R.; Savtchenko, R.; Ostapchenko, V. G.; Makarava, N.; Baskakov, I. V. *Biochemistry* **2010**, *49*, 9488.

Supporting Information

Intermolecular Alignment in Y145Stop Human Prion Protein Amyloid Fibrils Probed by Solid-State Nuclear Magnetic Resonance Spectroscopy

Jonathan J. Helmus,[†] Krystyna Surewicz,[‡] Marcin I. Apostol,[‡] Witold K. Surewicz,[‡] and Christopher P. Jaroniec[†,*]

[†]*Department of Chemistry, The Ohio State University, Columbus, Ohio 43210*
[‡]*Department of Physiology and Biophysics, Case Western Reserve University, Cleveland, Ohio 44106*

E-mail: jaroniec@chemistry.ohio-state.edu

Preparation of huPrP23-144 Amyloid Fibrils

Isotopically enriched and natural abundance huPrP23-144 was overexpressed in *Escherichia coli* BL21 Star™ (DE3) One Shot cells (Invitrogen) and purified as described previously.[1] The ^{13}C and/or ^{15}N labeled proteins were prepared using minimal medium containing the following additives,[2-4] ^{15}N-huPrP23-144: 1 g/L $^{15}NH_4Cl$, 4 g/L glucose; 1,3-^{13}C-huPrP23-144: 1 g/L $^{14}NH_4Cl$, 2 g/L $NaH^{12}CO_3$, 2 g/L [1,3-^{13}C]glycerol; 2-^{13}C-huPrP23-144: 1 g/L $^{14}NH_4Cl$, 2 g/L $NaH^{13}CO_3$, 2 g/L [2-^{13}C]glycerol; 1,3-^{13}C,^{15}N-huPrP23-144: 1 g/L $^{15}NH_4Cl$, 2 g/L $NaH^{12}CO_3$, 2 g/L [1,3-^{13}C]glycerol; 2-^{13}C,^{15}N-huPrP23-144: 1 g/L $^{15}NH_4Cl$, 2 g/L $NaH^{13}CO_3$, 2 g/L [2-^{13}C]glycerol. All ^{13}C and ^{15}N-enriched compounds were purchased from Cambridge Isotope Laboratories (Andover, MA).

Amyloid fibrils were formed at 25 ^{o}C without agitation for ~24 h by dissolving lyophilized huPrP23-144 in ultrapure water at a concentration of 5 mg/ml, followed by addition of pH 6.4 potassium phosphate buffer to a final concentration of 50 mM. Fibrils were characterized by atomic force microscopy to confirm sample homogeneity, pelleted by low-speed centrifugation, washed with several aliquots of 50 mM pH 6.4 potassium phosphate buffer, and centrifuged into Varian 3.2 mm limited-speed zirconia rotors for solid-state NMR analysis. The rotors contained ~15 mg of total protein and were sealed using custom-made spacers (Revolution NMR, Fort Collins, CO) to prevent sample dehydration during NMR experiments. A total of six samples were used in this study, corresponding to huPrP23-144 fibrils formed from: (1) 1,3-^{13}C,^{15}N-huPrP23-144, (2) a physical mixture of 1,3-^{13}C,^{15}N-huPrP23-144 and natural abundance huPrP23-144 in a 1:3 molar ratio, (3) a physical mixture of 1,3-^{13}C-huPrP23-144 and ^{15}N-huPrP23-144 in a 1:1 molar ratio, (4) 2-^{13}C,^{15}N-huPrP23-144, (5) a physical mixture of 2-^{13}C,^{15}N-huPrP23-144 and natural abundance huPrP23-144 in a 1:3 molar ratio, and (6) a physical mixture of 2-^{13}C-huPrP23-144 and ^{15}N-huPrP23-144 in a 1:1 molar ratio.

Solid-State NMR Spectroscopy

NMR experiments were carried out using a three-channel Varian spectrometer operating at the frequencies of 499.8 MHz for ^{1}H, 125.7 MHz for ^{13}C, and 50.6 MHz for ^{15}N, and equipped with 3.2 mm triple-resonance T3 and BioMAS[5] probes in ^{1}H-^{13}C-^{15}N configuration. All experiments employed MAS rates of 11.111 kHz, actively regulated to ca. ± 3 Hz using a Varian MAS control unit. Effective sample temperatures during the experiments were maintained at ~5 ^{o}C using a variable temperature stack and temperature control unit.

2D ^{15}N-^{13}C chemical shift correlation spectra for the huPrP23-144 fibril samples were acquired using the z-filtered TEDOR pulse scheme,[6] with $t_{1,max}(^{15}N) \approx 14$ ms, $t_{2,max}(^{13}C) \approx 24$ ms, 27.8 kHz ^{15}N recoupling pulses, 5.4 ms z-filter periods with simultaneous application of ~50 kHz continuous-wave ^{1}H

field to suppress undesirable antiphase and multiple-quantum coherences, and 100 kHz and 70 kHz TPPM ^{1}H decoupling[7] during the TEDOR mixing and chemical shift evolution/acquisition periods, respectively. The TEDOR mixing times, τ_{TEDOR}, employed ranged from 1.44 ms to 18.0 ms.

1D TEDOR trajectories that report simultaneously on all intermolecular ^{15}N-^{13}CO and ^{15}N-^{13}Cα distances in huPrP23-144 fibrils were recorded for the mixed 1,3-^{13}C/^{15}N and 2-^{13}C/^{15}N samples, respectively. For the ^{15}N-^{13}CO trajectory, a series of 30 ^{13}C 1D spectra were collected with τ_{TEDOR} varied between 0.72 ms and 21.6 ms in 0.72 ms increments—this set of experiments also employed a band-selective 360 μs rSNOB[8] ^{13}C refocusing pulse centered in the carbonyl region to suppress any residual ^{13}CO-^{13}Cα J-couplings.[6] For the ^{15}N-^{13}Cα trajectory, a series of 12 ^{13}C spectra were collected with τ_{TEDOR} varied between 1.8 ms and 21.6 ms in 1.8 ms increments.

Estimation of the β-Strand Spacing in huPrP23-144 Fibrils from Solid-State NMR Data

As discussed in the main text, the multiple intermolecular correlations observed in 2D ^{15}N-^{13}C TEDOR correlation spectra for the mixed 1,3-^{13}C/^{15}N and 2-^{13}C/^{15}N huPrP23-144 fibril samples (c.f., Figures 1 and S1) are consistent with a parallel in-register alignment of the β-strand segments within the amyloid core. The β-strand spacing was estimated by recording 1D TEDOR trajectories—that report on all intermolecular ^{15}N-^{13}CO and ^{15}N-^{13}Cα distances, respectively—for the mixed 1,3-^{13}C/^{15}N and 2-^{13}C/^{15}N fibril samples as described above, and comparing these experimental trajectories with ones calculated for model spin systems (c.f., Figure 2).

The simulated 1D TEDOR trajectories were generated using the SPINEVOLUTION program[9] as follows. First, a series of atomic coordinate files corresponding to model spin systems to be used by SPINEVOLUTION for the nuclear spin dynamics simulations was built based on the X-ray structure of amyloid-like microcrystals of the peptide GNNQQNY[10] displaying a parallel in-register alignment of the β-strands (PDB ID 2OMM), where the spacing between adjacent strands, *d*, (c.f., Figure 2) was varied between 3.5 and 6.0 Å in 0.1 Å increments. Next, for each β-strand spacing SPINEVOLUTION was used to calculate three different TEDOR buildup trajectories for a ^{13}CO or ^{13}Cα spin on the central strand (denoted as "0" in the structural models shown in Figure 2) arising from dipole-dipole couplings to ^{15}N nuclei located within 6 Å of the ^{13}CO/^{13}Cα spin on the adjacent "+1" and "-1" strands—specifically, the three trajectories corresponded to the ^{13}C nucleus coupled to: (1) two nearest-neighbor ^{15}N spins on strand "+1", (2) two nearest-neighbor ^{15}N spins on strand "-1", and (3) four nearest-neighbor ^{15}N spins on strands "+1" and "-1", indicated by spheres in the models in Figure 2. This was followed by averaging the three calculated trajectories in a 1:1:1 ratio, in accord with the ^{13}C-^{15}N spin topologies that are expected for amyloid fibrils grown from an isotropic 1:1 physical mixture of ^{13}C and

^{15}N-labeled protein monomers. Finally, the dependence of the data analysis on additional parameters not related to the β-strand spacing, including nuclear spin relaxation and overall spectral intensity, was eliminated as follows. First, the ^{13}CO/^{13}Cα intensities for the experimental TEDOR trajectories were scaled by the corresponding intensities in 1D cross-polarization ^{13}C reference spectra recorded under identical conditions. Second, the transverse ^{13}C spin relaxation rates were determined by standard spin-echo methods (under the experimental conditions of this study the collective ^{13}CO and ^{13}Cα relaxation rate constants for the mixed 1,3-^{13}C/^{15}N and 2-^{13}C/^{15}N huPrP23-144 fibril samples were found to be 82 s^{-1} and 136 s^{-1}, respectively) and subsequently used to scale the calculated TEDOR trajectories by a factor of $\exp\{-R_2 \times \tau_{TEDOR}\}$, where R_2 is the ^{13}CO/^{13}Cα transverse relaxation rate. Note that the effects of ^{13}C-^{13}C J-couplings on the spin dynamics are negligible for these TEDOR experiments due to the use of the sparse ^{13}C labeling scheme, which eliminates most one-bond ^{13}C-^{13}C J-couplings,[3,4] and/or the band-selective ^{13}C pulse for the ^{15}N-^{13}CO measurements. Thus, in summary simulations of the 1D TEDOR trajectories contained no adjustable parameters other than the β-strand spacing, *d*. For each value of *d* in the grid the root-mean-square deviation (RMSD) was determined between the experimental and simulated trajectories; *d* = 4.4 Å was found to give the lowest RMSD values for both the ^{15}N-^{13}CO and ^{15}N-^{13}Cα data sets (c.f., Figure 2).

X-ray Fiber Diffraction

Fibers were pelleted using low speed centrifugation, washed with water to eliminate salts, and re-pelleted. The pellet was subsequently resuspended with a small volume of water. The resuspened pellet was pipetted into a space between the ends of two glass rods. As the pellet dried, fibers aligned themselves between the rods. Diffraction images were collected at the Cleveland Center of Membrane and Structural Biology (CCMSB) using a Rigaku MicroMax-007HF copper anode X-ray source and a Rigaku Saturn 944+ CCD detector.

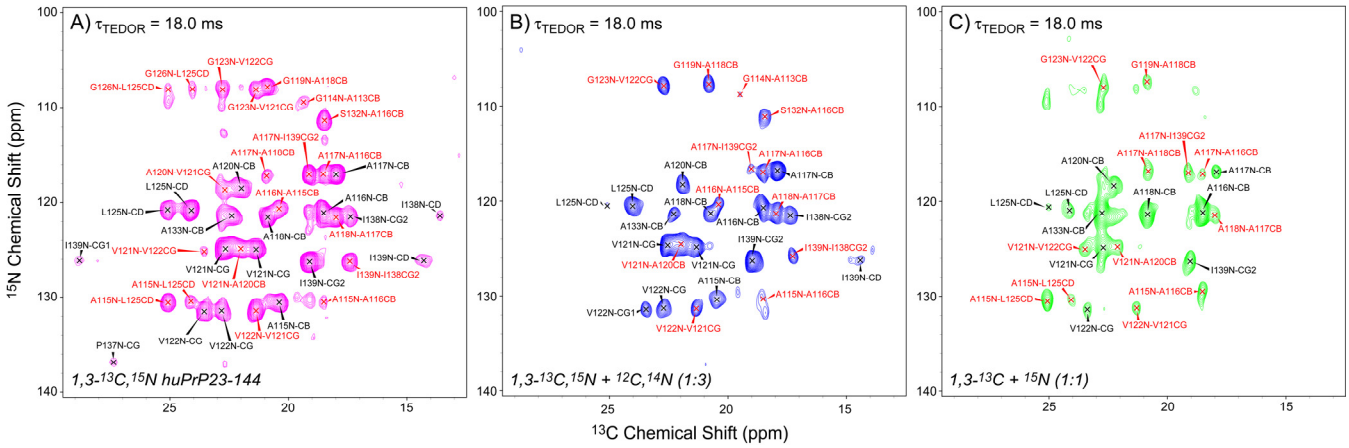

Figure S1. Regions of ^{15}N-^{13}CX (NCX) TEDOR correlation spectra corresponding to side-chain methyl ^{13}C for huPrP23-144 fibrils. The spectra were recorded at 500 MHz ^{1}H frequency, 11.111 kHz MAS rate and effective sample temperature of ~5 ^{o}C using the *z*-filtered TEDOR pulse scheme with ^{15}N-^{13}C dipolar mixing times, τ_{TEDOR}, indicated in the spectra for amyloid fibril samples prepared from (A) 1,3-^{13}C,^{15}N-huPrP23-144, (B) a mixture of 1,3-^{13}C,^{15}N-huPrP23-144 and natural abundance huPrP23-144 in a 1:3 molar ratio, and (C) a mixture of 1,3-^{13}C-huPrP23-144 and ^{15}N-huPrP23-144 in a 1:1 molar ratio. The experiment times for spectra in panels (A-C) were ~66, ~108 and ~212 h, respectively. The intra-residue ^{15}N-^{13}C correlations that are relevant to the current study are labeled in black font. Inter-residue correlations are labeled in red font.

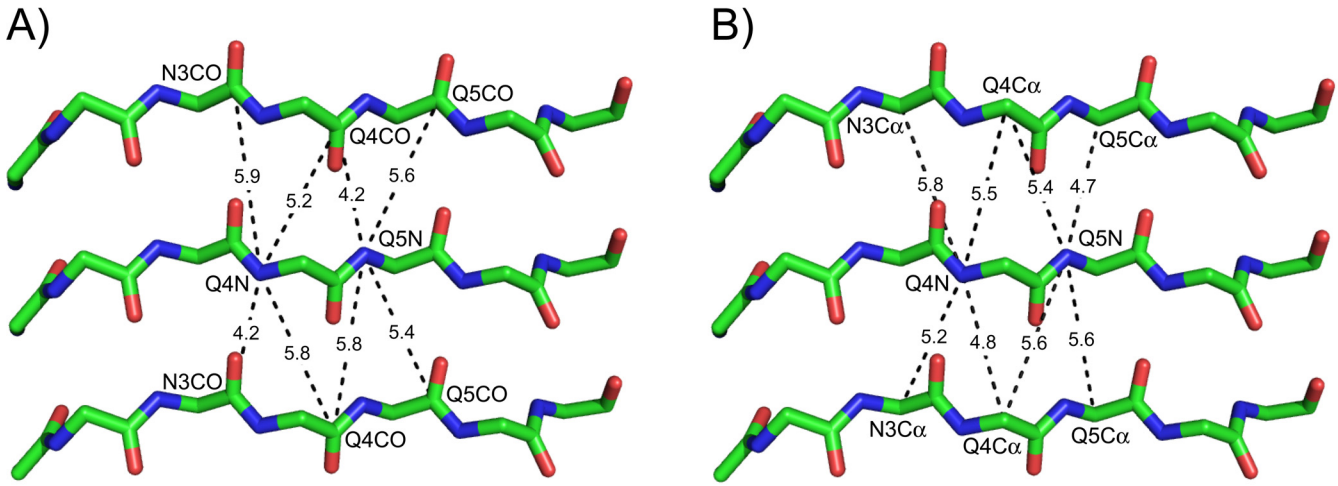

Figure S2. Typical nearest-neighbor and next-nearest-neighbor intermolecular (A) ^{15}N-^{13}CO and (B) ^{15}N-^{13}Cα distances (in Å) for amyloid-like microcrystals of the model peptide GNNQQNY displaying a parallel in-register alignment of the β-strands (PDB ID 2OMM).[10] All other intermolecular ^{15}N-^{13}C distances were > 6 Å. Side-chain atoms are not shown for clarity.

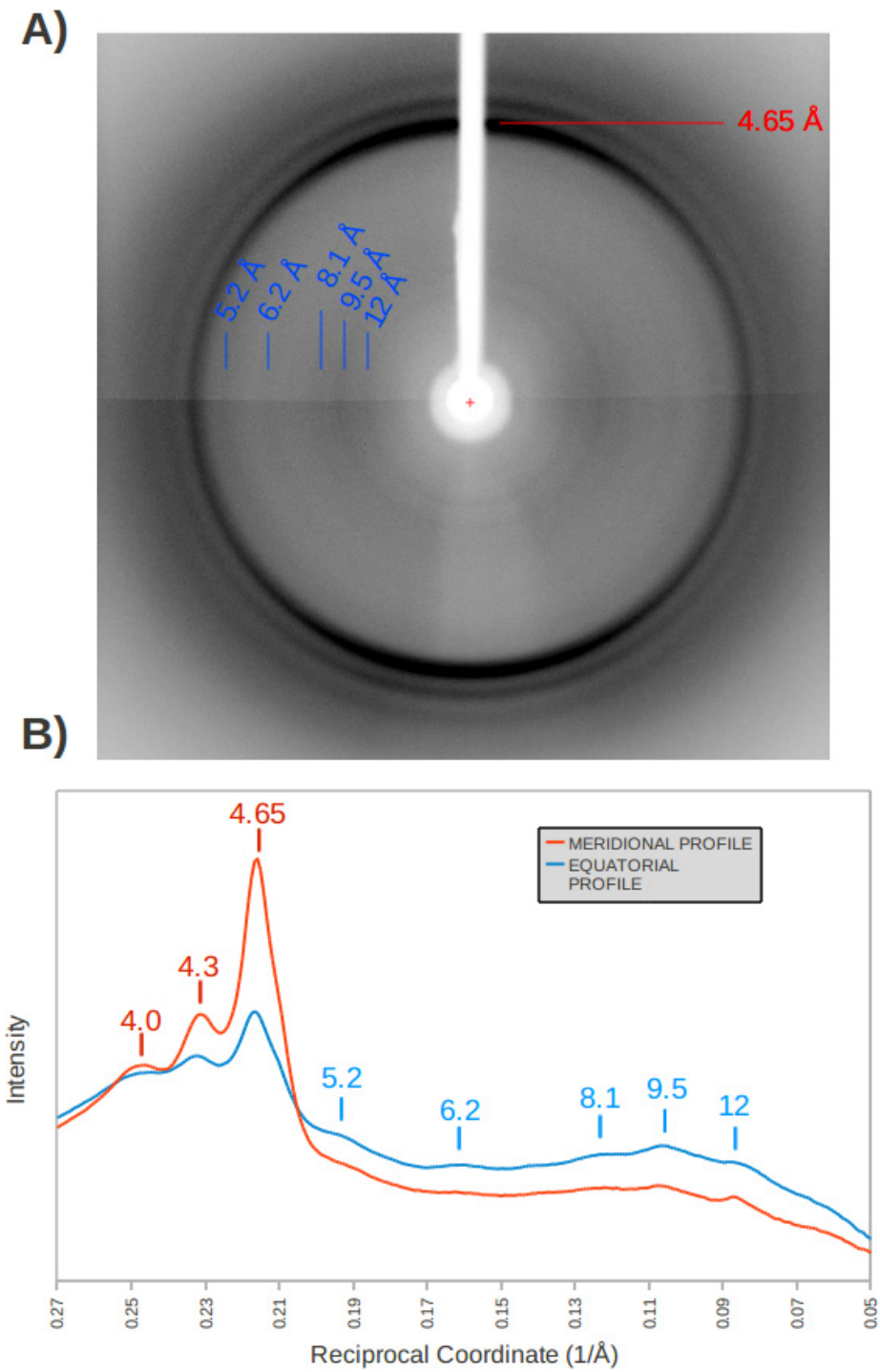

Figure S3. X-ray diffraction of aligned huPrP23-144 fibrils. (A) The X-ray diffraction image shows a pattern with a prominent 4.65 Å reflection along the meridional or fiber axis corresponding to the spacing between β-strands along this axis. There are also five weak equatorial reflections at 5.2, 6.2, 8.1, 9.5 and 12 Å arising from the spacing between stacks of β-sheets within the fiber structure. (B) A graphical comparison of the intensity of the reflections along the meridian (red) and equator (blue) of the fiber diffraction pattern with peaks labeled above in units of Å.

References

(1) Helmus, J. J.; Surewicz, K.; Nadaud, P. S.; Surewicz, W. K.; Jaroniec, C. P. *Proc. Natl. Acad. Sci. USA* **2008,** 105, 6284-6289.

(2) Cai, M. L.; Huang, Y.; Sakaguchi, K.; Clore, G. M.; Gronenborn, A. M.; Craigie, R. *J. Biomol. NMR* **1998,** 11, 97-102.

(3) LeMaster, D. M.; Kushlan, D. M. *J. Am. Chem. Soc.* **1996,** 118, 9255-9264.

(4) Castellani, F.; van Rossum, B.; Diehl, A.; Schubert, M.; Rehbein, K.; Oschkinat, H. *Nature* **2002,** 420, 98-102.

(5) Stringer, J. A.; Bronnimann, C. E.; Mullen, C. G.; Zhou, D. H. H.; Stellfox, S. A.; Li, Y.; Williams, E. H.; Rienstra, C. M. *J. Magn. Reson.* **2005,** 173, 40-48.

(6) Jaroniec, C. P.; Filip, C.; Griffin, R. G. *J. Am. Chem. Soc.* **2002,** 124, 10728-10742.

(7) Bennett, A. E.; Rienstra, C. M.; Auger, M.; Lakshmi, K. V.; Griffin, R. G. *J. Chem. Phys.* **1995,** 103, 6951-6957.

(8) Kupce, E.; Boyd, J.; Campbell, I. D. *J. Magn. Reson. B* **1995,** 106, 300-303.

(9) Veshtort, M.; Griffin, R. G. *J. Magn. Reson.* **2006,** 178, 248-282.

(10) Sawaya, M. R.; Sambashivan, S.; Nelson, R.; Ivanova, M. I.; Sievers, S. A.; Apostol, M. I.; Thompson, M. J.; Balbirnie, M.; Wiltzius, J. J.; McFarlane, H. T.; Madsen, A. Ø.; Riekel, C.; Eisenberg, D. *Nature* **2007,** 447, 453-457.